

2-8-2021

Single-particle crushing test and numerical simulation of coarse grained soil based on size effect

Min-qiang MENG

School of Civil Engineering, Chongqing University, Chongqing 400045, China

Lei WANG

School of Civil Engineering, Chongqing University, Chongqing 400045, China

Xiang JIANG

School of Civil Engineering, Chongqing University, Chongqing 400045, China

Cheng-gui WANG

School of Civil Engineering, Chongqing University, Chongqing 400045, China

See next page for additional authors

Follow this and additional works at: <https://rocksoilmech.researchcommons.org/journal>



Part of the [Geotechnical Engineering Commons](#)

Custom Citation

MENG Min-qiang, WANG Lei, JIANG Xiang, WANG Cheng-gui, LIU Han-long, XIAO Yang, . Single-particle crushing test and numerical simulation of coarse grained soil based on size effect[J]. Rock and Soil Mechanics, 2020, 41(9): 2953-2962.

This Article is brought to you for free and open access by Rock and Soil Mechanics. It has been accepted for inclusion in Rock and Soil Mechanics by an authorized editor of Rock and Soil Mechanics.

Single-particle crushing test and numerical simulation of coarse grained soil based on size effect

Authors

Min-qiang MENG, Lei WANG, Xiang JIANG, Cheng-gui WANG, Han-long LIU, and Yang XIAO

Single-particle crushing test and numerical simulation of coarse grained soil based on size effect

MENG Min-qiang¹, WANG Lei¹, JIANG Xiang¹, WANG Cheng-gui¹, LIU Han-long^{1, 2, 3}, XIAO Yang^{1, 2, 3, 4}

1. School of Civil Engineering, Chongqing University, Chongqing 400045, China

2. Key Laboratory of New Technology for Construction of Cities in Mountain Area, Chongqing University, Chongqing 400045, China

3. National Joint Engineering Research Center of Geohazards Prevention in the Reservoir Areas (Chongqing), Chongqing 400045, China

4. State Key Laboratory for Geomechanics & Deep Underground Engineering, China University of Mining & Technology, Xuzhou, Jiangsu 221116, China

Abstract: The coarse-grained soil is prone to particle breakage under external loads and other factors. A series of single-particle fragmentation tests is conducted for mudstone and sandstone particles. Based on the size effect and fractal model of particle fragmentation, the relationships between the fractal dimension and single-particle crushing strength, fragmentation energy, and Weibull modulus are investigated. A single particle crushing process is analyzed using PFC^{3D} and the modelling results are compared with that from the experimental data to verify the reliability of numerical code. The crushing strength and crushing energy of large particle size are then analyzed by numerical models. The results show that the fractal dimensions of different materials are different under the same test conditions. The fragmentation degree of sandstone with different grain sizes is greater than that of mudstone. The crushing strength of a single particle has an obvious size effect. In addition, the crushing strength and energy of single particle can be predicted by fractal dimension and particle size. The modified Weibull modulus can be also predicted by fractal dimension. The numerical simulation results agree with the experimental results and also agree with the predicted results. Besides, the modelling results of the single particle crushing strength with large particle size are also consistent with the predicted results. The crushing energy, however, shows slightly different, which requires further experimental verification. The research results can provide a reference for obtaining the single particle strength and deformation characteristics of large-size coarse-grained soil.

Keywords: size effect; fractal dimension; single-particle crushing strength; crushing energy; Weibull distribution; numerical simulation

1 Introduction

The coarse-grained soil has been widely used in many engineering projects, especially for the dam and railway projects^[1–4] due to its advantages of high strength, small deformation, good permeability, and easy-obtained materials. The coarse-grained soil will show obvious particle fragmentation under external load and the particle breakage will change the initial particle size distribution curve, which can largely affect the strength and deformation features of coarse-grained soil^[5–6]. Currently, however, the coarse-grained soil used in engineering projects are normally associated with large size, which leads to the difficulty for studying the macro-mechanics and deformation characteristics in laboratory experiments^[7]. In this consideration, it is of great engineering significance to study the single particle crushing strength and size effect of coarse-grained soil.

To study the size effect of coarse-grained soil, based on the fracture mechanics theory, Frossard et al^[8] proposed a reasonable method for evaluating the failure strength of rockfill material and they also conducted experimental

tests to verify the accuracy of the proposed evaluation method. Zhou et al^[6] conducted numerical simulations of single particle crushing on five groups of rockfill material with different particle sizes. They found that the crushing strength of different particle sizes had an obvious size effect. In recent years, many scholars have performed researches on the crushing characteristics and mechanical properties of single particles of granular material using laboratory tests. Nakata et al^[9] conducted single particle crushing tests on the quartz and feldspar minerals of Aio sand. They found that the crushing force–displacement curve of quartz particle increased monotonously, while the force–displacement of feldspar particle showed a zigzag increasing trend. They also found the Weibull modulus was also different for various mineral particles. McDowell et al.^[10] and Lim et al^[11] conducted single particle crushing tests to study the crushing strength of different particle sizes of Quiou sand and rail ballast. They concluded that the distribution of particle crushing strength followed a Weibull distribution and there was a power function relationship between the crushing strength and particle size. Using a high-speed microscope camera to capture

Received: 25 November 2019

Revised: 19 March 2020

This work was supported by the National Natural Science Foundation of China(51922024, 51509024); the Fundamental Research Funds for the Central Universities (2019CDXYTM0033) and the State Key Laboratory for Geomechanics & Deep Underground Engineering, China University of Mining & Technology (SKLGDUEK1810).

First author: MENG Min-qiang, male, born in 1991, PhD candidate, mainly engaged in the research on particle crushing characteristics of coarse-grained soil. E-mail: mengmq19911206@163.com

Corresponding author: XIAO Yang, male, born in 1982, PhD, Professor, mainly engaged in the research on the mechanical features and constitutive model of coarse-grained soil. E-mail: hhuxyanson@163.com

the crushing process, Wang et al.^[12] conducted single particle crushing tests on Leighton Buzzard sand and fully weathered granite particles. They found that the single particle crushing modes can be divided into four types and the soaking has little effect on the failure model of single particle.

Based on previous research results, in this study, the size distribution of single particle after crushing was first determined using a screening test, and the fractal dimension was calculated based on a fractal model. Based on the test results, the size effect of particle crushing strength was then studied and the relations among particle crushing strength, crushing energy, and fractal dimension were discussed. The Weibull modulus was compared and analyzed before and after correction. Besides, the DEM numerical software PFC^{3D} was used to simulate the single particle crushing process. The modelled results were compared with that of the test results and the predicted results to verify the reliability of the numerical simulation. In addition, the numerical modelling was extended to large particle size. The crushing strength and crushing energy were analyzed to provide a reference for obtaining the strength and deformation of large size coarse-grained soil.

2 Single particle crushing test and discrete element modelling

2.1 Single particle crushing test

The single particle crushing tests are conducted using the micro-test materials testing module (MMTM) produced by British Deben Company, as shown in Fig. 1(a)–Fig. 1(c). Figure 1(a) shows the main module of the test instrument. Figure 1(c) shows the main controller of the test instrument, which can record the force and compression displacement in real-time. The maximum load is 5 kN with 0.01 N accuracy. The data acquisition interval of instrument is 0.1–5.0 s and can record up to 256 000 data points. In this study, the data acquisition interval was set as 0.1 s. The loading rate of the instrument can be 0.1, 0.2, 0.5, 1.0, and 1.5 mm/min. To ensure the test accuracy, the loading rate was selected as 0.1 mm/min in this study.

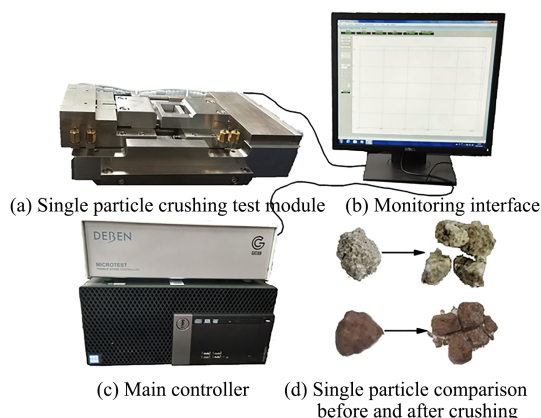


Fig. 1 Material micro-test testing system

In this study, the test materials were mudstone and sandstone. The mudstone was sampled from a railway construction site in Chongqing, China. The relative density $G_s = 2.76$. The sandstone was taken from a large quarry in Chongqing with a relative density of $G_s = 2.69$. The test samples were dried (105 °C, 24 h) and then reserved. McDowell et al.^[10] found that the particle shape must be the same or similar when the Weibull distribution was used to statistic particle strength. The mudstone and sandstone particles were subjected to the screening tests. Three particle sizes of 2.5, 5.0, and 10.0 mm were selected. For each particle size, the number of particles was selected as 30 and the particle shape was similar. The tests were terminated when the particles were broken into 3 to 4 pieces. Figure 1(d) shows the particle morphology comparison between the 5 mm sandstone and mudstone samples before and after the crushing tests.

2.2 DEM modelling

Since 1979, after Cundall et al.^[13] proposed a discrete element method that suitable for soil mechanic, this DEM method has been widely promoted and applied in geo-technical engineering^[14–18]. In this study, DEM numerical software of PFC^{3D} with explicit difference algorithm that developed by Itasca Consulting Company is used herein for the particle flow modelling. For simplicity, as shown in Fig. 2, the single particle is assumed as spherical shape, which simulates a breakable particle by bonding a certain number of sub-particles to form a cluster. The sub-particles are generated according to a certain particle size distribution. The bottom is a smooth flat plate and is fixed in the modelling. The load is applied by a falling weight that composed of rigid small balls without stress and deformation among each other. The bottom of the falling weight is also smooth. A linear contact model is set for contacts among the falling weight and the single particle, the bottom plate. A parallel bonding model is used for the contacts among the small balls for the single particle, and the particle contact degenerate into a linear contact model after the particle is broken. It should be mentioned that the size effect of material elastic parameter is not considered in this study. The elastic moduli of mudstone and sandstone are 3.1 and 2.3 GPa, respectively. The densities of mudstone and sandstone are 2.76 and 2.69 g/cm³. The Poisson's ratio is assumed to be 0.3. The porosity of the generated single particle is 0.3 and the friction coefficient is 0.58. The bond strength among the sub-particles follows a normal distribution. The mean value and variance of the bond strength of the 2.5 mm particles are obtained by comparing that with the experimental data. The bonding strength of the remaining particles is then calculated from the strength relation of the size effect that derived from the experiments. Once the bond of sub-particle is broken, the single particle sphere is then failed^[19]. The total number of balls is probably controlled to about 600 to ensure a proper calculation speed of the numerical modelling.

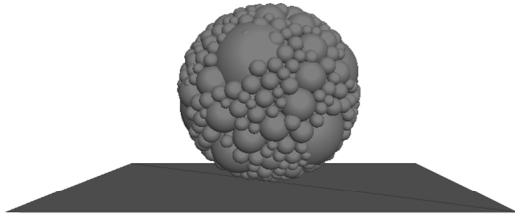


Fig. 2 A typical DEM model of a single particle

3 Fractal dimension of single particle

3.1 Fractal model of single particle

Since the 1970 s, the fractal theory proposed by Mandelbrot^[20] has been widely used to describe the self-similarity between parts and the whole things^[21]. The fractal dimension D can be obtained by crushing tests. In different crushing tests of the same material, the fractal dimension of particles is also different. The fractal dimension determined by the same test of the same material can be used to predict the mechanical properties of the same material^[22].

According to the fractal theory^[23–24], the particle size distribution curve follows the fractal distribution. Based on the research of Einav^[25]:

$$F(d) = \left(\frac{d}{d_M} \right)^{3-D} \quad (1)$$

where $F(d)$ is the mass content percentage of particles with particle size less than d ; d_M is the maximum particle size. From Eq.(1), D can be derived:

$$D = 3 - \alpha \quad (2)$$

where α is the slope of the relation between $F(d)$ and d/d_M in a double logarithmic coordinate.

3.2 Test results analysis

A typical crushing force–displacement relation of single particle coarse-grained soil is shown in Fig.3. The curve shows a zigzag shape, which is because the edges and corners of the test sample are broken locally at the initial stage of loading. The crushing force hence increases firstly and then decreases afterwards. When the applied load reaches the maximum load that the sample can be borne, the main sample body is failed and the force reaches the maximum value, which is as the breaking point. Afterwards, the displacement continues to increase, and the force decreases in the post-peak stage until the sample is broken into 3–4 pieces. The process was analyzed in more details in the literatures^[26–27] and will not repeat here. The crushing energy is shown as the shaded area in Fig.3^[28].

After the test sample was crushed, the crushed particle pieces of various sizes were collected and sieved to determine the particle size distribution, as shown in Fig.4.

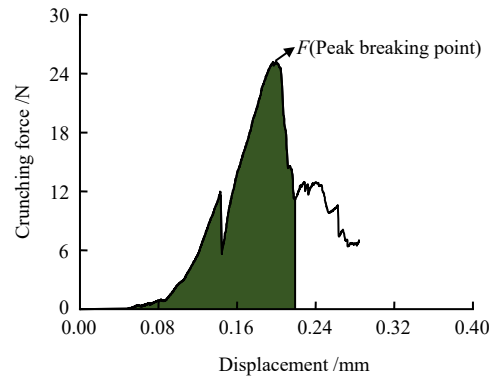
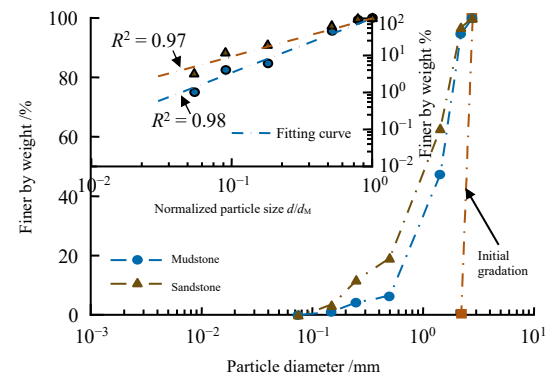
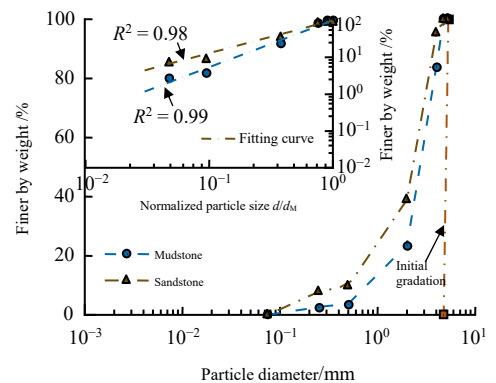


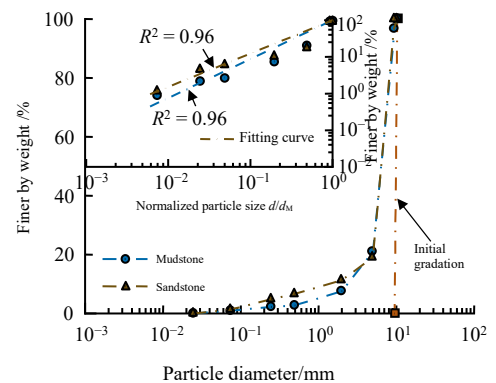
Fig. 3 A typical force–displacement curve of a single particle



(a) 2.5 mm



(b) 5.0 mm



(c) 10.0 mm

Fig. 4 Particle size distribution and fractal dimension for the single particle crushing tests
As can be seen from Fig.4, there are three single particle

tests with different sizes. Due to the breaking of particle, the particle size distribution curves of mudstone and sandstone move to the upper left portion of the coordinate system, and the sandstone fragmentation is larger than that of the mudstone. This is because the strength of mudstone is relatively higher than that of the sandstone under the dry condition. It is also can be seen from the Fig.4 that the particle size distribution curves of mudstone and sandstone are also presented in a double logarithmic coordinate. For different initial particle sizes, the fractal dimension of mudstone is smaller than that of sandstone, and the fractal dimensions of two samples decrease as the particle size decreases. However, as the particle size decreases, the fractal characteristics become obviously, and the gradation distribution is wider. This is mainly caused by that the sample with smaller particle size is broken completely after reaching the peak strength when compared that with the sample associated with larger particle size. The smaller particle size after crushing, the stronger the fractal characteristics.

For the same test material, the particles of three particle sizes were uniformly mixed together and then conducted a sieving test to obtain a particle size distribution curve, as shown in Fig.5. The slopes of the particle size distribution curves of mudstone and sandstone are 0.86 and 0.78 on the double logarithmic coordinate, respectively. Under the test condition of single particle crushing, according to Eq.(2), the ultimate fractal dimensions of mudstone and sandstone are $D_{mudstone}=2.14$ and $D_{sandstone}=2.22$, respectively. In the DEM numerical simulation, the gradation of sub-particles of the single particle is determined according to Eq.(1) and the fractal dimension D that determined by the experimental tests.

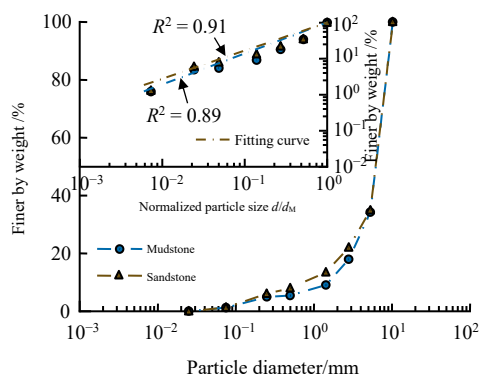


Fig.5 Particle size distribution and ultimate fractal dimension for the single particle crushing tests

4 Crushing strength and crushing energy of single particle

4.1 Strength theory of single particle crushing

To study the surface breaking strength of ice particles, based on Jaeger^[30] study, Xu et al^[22, 24, 29] proposed a formula to determine the ice particle breaking strength

σ_f :

$$\sigma_f = \frac{F}{A_{app}} \tag{3}$$

where A_{app} is the particle cross-sectional area perpendicular to the F direction, $A_{app} = d^2$; F is the crushing force. Assume the inherent tensile strength σ_f^* of the particle is a fixed value, then

$$\left. \begin{aligned} \sigma_f &= \sigma_f^* d^{D-3} \\ \sigma_f^* &= \frac{\sum_{i=1}^n \sigma_{fi} d_i^{3-D}}{n} \end{aligned} \right\} \tag{4}$$

where n is the number of measured test data; σ_{fi} is the tensile strength of the particle corresponding to the particle size d_i .

4.2 Energy theory of single particle crushing

According to the work definition, the crushing energy is defined as the product of crushing force and compression displacement. Then

$$E_f = \int_0^{\Delta} F d\Delta \tag{5}$$

where E_f is the single particle crushing energy; Δ is the compression displacement.

According to the elastic theory, there is a functional relation between the compression displacement Δ of a single particle and the crushing force F :

$$\Delta \propto F^{\frac{2}{3}} \tag{6}$$

It can be obtained by combing the Eqs. (3)–(6):

$$E_f \propto d^{\frac{5D-2}{3}} \tag{7}$$

4.3 Test results analysis

Based on the theory of single particle crushing strength of ice particles, it is known that the single particle crushing strength of mudstone and sandstone can be calculated from Jaeger^[30] in the tests. Xiao et al^[26] concluded that the crushing strength of the same sandstone particle size is also different due to the differences in its shape and internal cracks. In addition, the mudstone has similar characteristics^[27]. Hence, the average single particle crushing peak strength can be used to represent the single particle crushing strength in this study. The single particle crushing strengths of mudstone and sandstone are shown in Fig.6. It is seen from the Fig.6 that the strength of single particle mudstone with various particle sizes is higher than that of the single particle sandstone with the corresponding particle sizes. Similar conclusions can also be obtained from Fig.4. As the particle size increases, from Fig.6, the breaking strength of single particle decreases for both the mudstone and sandstone. When the particle diameter is 2.5 mm, the crushing strengths are 12.53 and

7.32 MPa for the mudstone and sandstone, respectively. When the particle diameter is 10 mm, however, the crushing strengths of mudstone and sandstone are 3.89 and 1.98 MPa, corresponding to a strength decrease of 69% and 73%, respectively. This demonstrates the size effect of the crushing strength of a single particle.

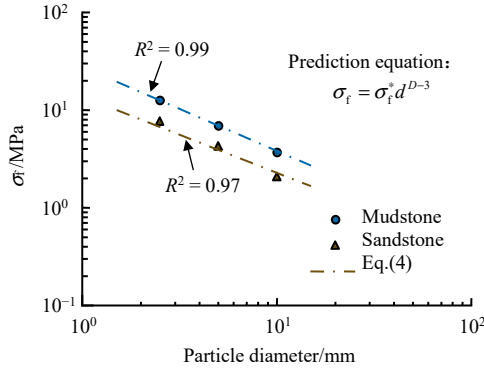


Fig. 6 Size effect of the single particle crushing strength

From Section 3.2, it is found that the fractal dimensions of mudstone and sandstone are $D_{\text{mudstone}} = 2.14$ and $D_{\text{sandstone}} = 2.22$, with the $3 - D$ values of 0.86 and 0.78, respectively. According to the test data and Eqs.(4) and (2), it is seen that the internal tensile strength of mudstone and sandstone are 27.7 and 13.75 MPa, respectively. Substituting into the first formula of Eq.(4), the prediction results are consistent with the test results. The correlation coefficients of the prediction data and the test data are $R^2_{\text{mudstone}} = 0.99$ and $R^2_{\text{sandstone}} = 0.97$ for the mudstone and sandstone, respectively. Therefore, the crushing strength of a single particle with a larger particle size can be then predicted by the particle fractal dimension D and Eq.(4).

The crushing energy of single particle can be estimated based on Eq.(5) and Fig.3. Like the crushing strength of single particles, even single particles with the same size and similar shape have different crushing energy. The average crushing energy of single particle is hence used to represent the single particle crushing energy in this study. From Fig.7, the crushing energy of single mudstone particle with same particle size is higher than that of the sandstone. This is because the mudstone can subject a higher crushing force than that of the sandstone. It can also be seen from Fig.7 that the crushing energy of single particle increases as the particle size increases. When the particle diameter is 2.5 mm, the crushing energy are 7.92 and 4.50 mJ for the mudstone and sandstone, respectively. When the particle diameter is 10 mm, the crushing energy of mudstone and sandstone can reach up to 239.65 and 74.74 mJ, corresponding to an energy increasing of 2529.88% and 1 560.89%, respectively. This means that the larger the particle size, the greater the energy stored inside, and the greater the energy released

when fragmentation occurs.

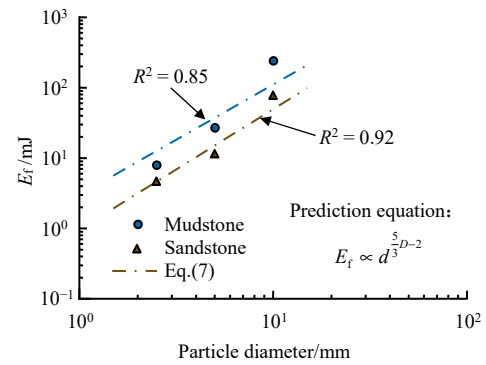


Fig. 7 The single particle crushing energy

From Eq.(7) and Fig.7, it can be seen that there is a power function relation between the crushing energy and the particle size of a single particle. In the double logarithmic coordinate system, the relation is a straight line and the slope is $5D/3 - 2$. The theoretical prediction value of single particle crushing energy can be derived from Eq.(7) and the predicted value is compared to the test data. It is found that the predicted value is consistent with the test data. The correlation coefficients of the theoretical prediction value and the laboratory test value are $R^2_{\text{mudstone}} = 0.85$ and $R^2_{\text{sandstone}} = 0.92$ for the mudstone and sandstone, respectively. In this way, the crushing energy of a single particle with a larger particle size can be predicted by the particle fractal dimension D and Eq.(7).

5 Weibull distribution of single particle

5.1 Modified Weibull distribution

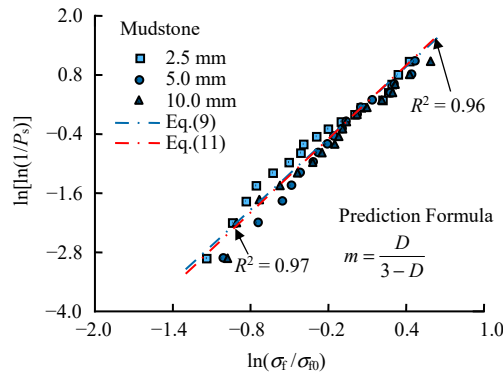
Since the Weibull distribution^[31] was proposed, it has been widely used to describe the breaking strength of brittle materials^[32–34]. For granular materials under the stress condition, the survival probability of particles P_s can be expressed as

$$P_s = \exp \left[- \left(\frac{d}{d_0} \right)^3 \left(\frac{\sigma}{\sigma_0} \right)^m \right] \quad (8)$$

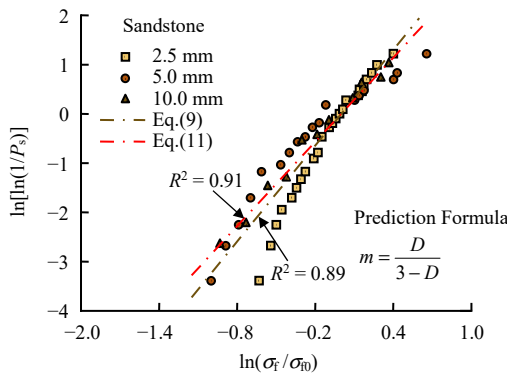
where P_s is the survival probability of particles; d_0 is the reference particle size; σ is the tensile stress of the granular material; σ_0 is the characteristic stress corresponding to the 37% survival probability of the granular material; m is the Weibull modulus. The larger the m , the smaller the dispersion of the particle strength^[21]. Eq.(8) gives the relation between tensile stress and survival probability.

When $d = d_0$, the relation between the survival probability and Weibull modulus can be expressed as

$$\ln \left[\ln \left(\frac{1}{P_s(d)} \right) \right] = m \ln \left(\frac{\sigma}{\sigma_0} \right) \quad (9)$$



(a) Weibull distribution of single particle strength of mudstone



(b) Weibull distribution of single particle strength of sandstone

Fig. 8 Weibull distributions of the single particle crushing strength

As for fractal particles, the survival probability of particles in Eq.(8) can also be^[35]

$$P_s = \exp \left[- \left(\frac{d}{d_0} \right)^D \left(\frac{\sigma}{\sigma_0} \right)^m \right] \quad (10)$$

where $\left(\frac{d}{d_0} \right)^D \left(\frac{\sigma}{\sigma_0} \right)^m = \text{constant}$. The σ is replaced by σ_f and combined with Eq.(4), then

$$m = \frac{D}{3 - D} \quad (11)$$

Eq.(11) is the modified Weibull modulus calculation equation.

5.2 Test results analysis

In this study, the survival probability P_s is calculated firstly by using the method proposed by Nakata et al^[36] and the Weibull modulus is obtained by using Eq.(9). As presented in Fig.8, the Weibull modulus of mudstone and sandstone are 2.42 and 3.24, respectively. Details about the calculation procedure of the Weibull modulus of mudstone and sandstone can be found in the references^[26–27]. Then, based on the obtained fractal dimension D of mudstone and sandstone, the modified Weibull modulus of the two samples can be then calculated using Eq.(11). The modified Weibull modulus are 2.49 and 2.85 for

the mudstone and sandstone, respectively.

Using Eqs.(9) and (11) to calculate the Weibull modulus, it is seen from Fig.8 that the Weibull modulus m of mudstone is increased by 2.89%, while the Weibull modulus m of sandstone is decreased by 12.04%. The two calculated results agree with each other. From Eq.(11), the correlation coefficients of the Weibull modulus are 0.97 and 0.91 for the mudstone and sandstone, respectively, which are slightly larger than those based on Eq.(9) (0.96 and 0.89 for the mudstone and sandstone). It is therefore to quickly calculate the Weibull modulus of granular materials by using the particle fractal dimension D and Eq.(11).

6 DEM numerical simulation

6.1 DEM numerical simulation procedure

From the analysis of Section 4.3, it is seen that the average crushing strength and energy of the large particle size can be predicted based on the fractal dimension D and Eqs.(4) and (7). In this section, the PFC^{3D} of DEM numerical software is used to simulate the crushing strength of every single particle with a 2.5 mm particle size. The modelling results are then compared to the laboratory test data to determine its bonding strength. Subsequently, based on Eq.(12)^[8] and the test results of single particle with particle size of 5.0 and 10 mm to determine the reliability of the selected input parameters. The selected parameters are further extended to single particles with larger sizes. Using the programmed code and the selected model parameters, the crushing strength of single particle is modelled with a size of 50, 100, and 200 mm. The average crushing strength is then obtained based on the modelling results. The modelled results are then compared with the crushing strength and energy that predicted by the Eqs.(4) and (7), so as to obtain the single particle crushing strength and energy of larger particle size:

$$\sigma_B = \left(\frac{d_B}{d_A} \right)^{-3/m} \sigma_A \quad (12)$$

where d_A and d_B are the particle sizes of the two known particles, respectively.

Figures 9 and 10 show the stress–strain curve of a single particle and the fragmentation process during the numerical modelling. In figure 9, a is a state without loading of the particle, which corresponds to the state a in Fig.10. The particle is then subjected to loading and the stress and strain are increased gradually, while the particle shape and stress state are not changed greatly, as state b shown in Figs.9b and 10b. After the particle is loaded for a period, as state c shown in Fig.9, some cracks begin to occur and the first peak point c appears on the stress–strain curve, which corresponds to state c in the Fig.10. After the first peak stress point appears, the particle starts to break (state d in Figs.9 and 10) and

the second peak stress point e appears on the stress–strain curve (state e in Figs.9 and 10). After the peak stress point, the particle continues to break into a fully crushed sample until 3 to 4 pieces of particle are formed, as states f–i shown in Figs.9 and 10.

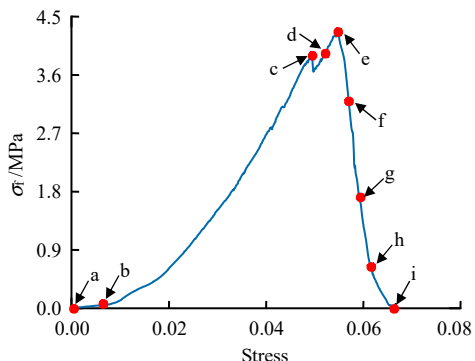


Fig. 9 Stress–strain curve of a single particle crushing model

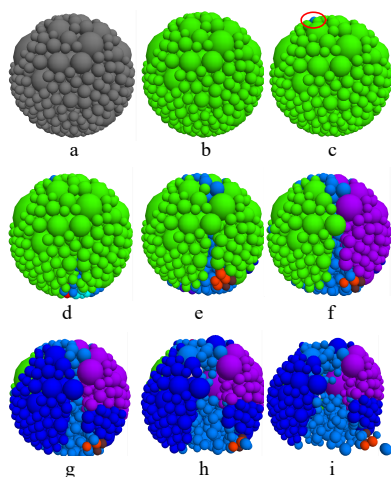
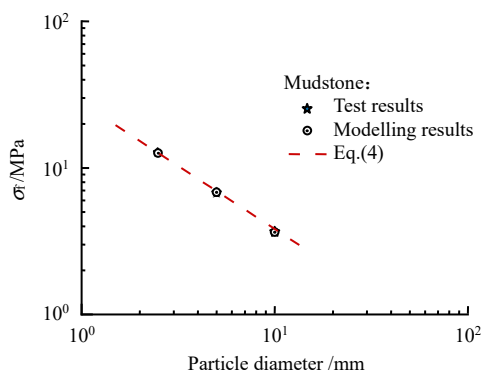


Fig. 10 Crushing process of a single particle model

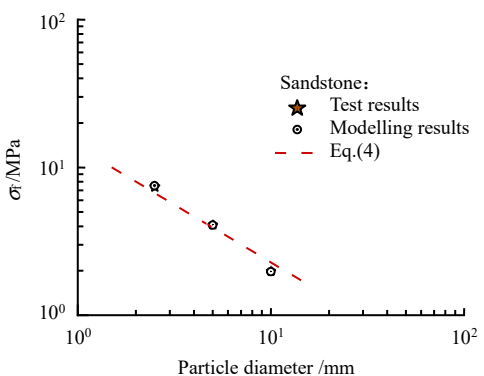
6.2 Comparative analysis of lab test, numerical, and theoretical results

From the PFC^{3D} modelling results, the average crushing strengths are determined for the single particle with 2.5, 5.0, and 10 mm sizes. The modelling results are compared to the laboratory test results and the prediction results from Eq.(4), as shown in Fig.11. The comparison of the average crushing strength of mudstone and sandstone is shown in Fig.11a and Fig.11b, respectively. For single particles with different sizes, it is found that the average crushing strengths based on the three methods (laboratory test, numerical modelling, and theoretical prediction Eq.(4)) are close to each other. For single particles, it is hence safe to conclude that the input model parameters are reasonable, and the numerical modelling can be used to estimate the crushing strength of larger particle size.

As shown in Fig.12, the comparison of the average crushing energy of mudstone and sandstone is shown in Figs.12a and 12b, respectively. As can be seen from Fig.12 that the average crushing energy shows small variations from the three estimation methods of laboratory

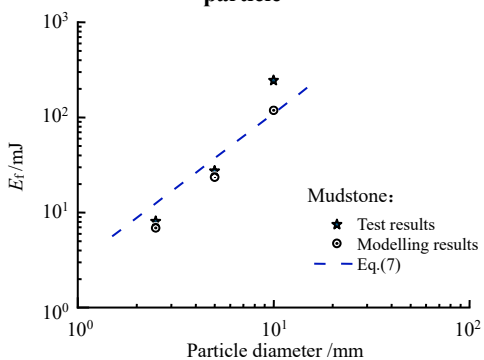


(a) Average crushing strength comparison of the mudstone single particle

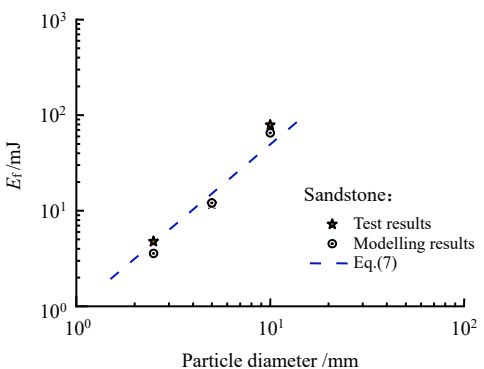


(b) Average crushing strength comparison of the sandstone single particle

Fig. 11 Average crushing strength comparison of the single particle



(a) Average crushing energy comparison of the mudstone single particle



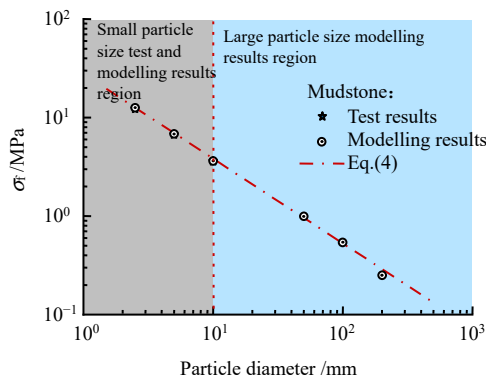
(b) Average crushing energy comparison of the sandstone single particle

Fig. 12 Average crushing energy comparison of the single particle

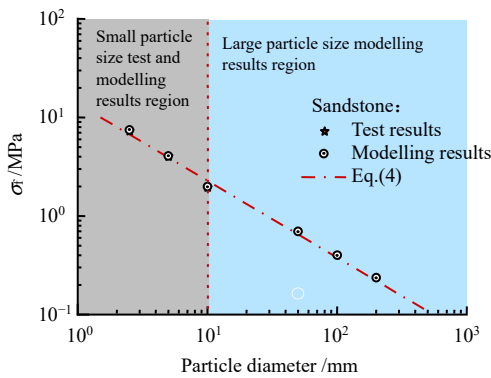
test, numerical modelling, and theoretical prediction Eq.(7). It is found that the larger the particle size, the greater the difference among the laboratory test results and the numerical modelling and the theoretical results. This is because of the randomness of the laboratory tests and the differences in the shape, size, and mineral content between the particles, which leads to the small variations of energy released during the tests. From an overall point of view, however, there is a little difference in the crushing energy estimated from the three methods. Hence, the crushing energy of large particle size can also be obtained using numerical modelling.

6.3 DEM modelling of large particle size

Eq.(12) and PFC^{3D} of DEM numerical code are used to obtain the crushing results of large particles with single particle sizes of 50, 100, and 200 mm, as shown in Figs.13 and 14.



(a) Average crushing strength comparison between the modelling and prediction results of the mudstone single particle



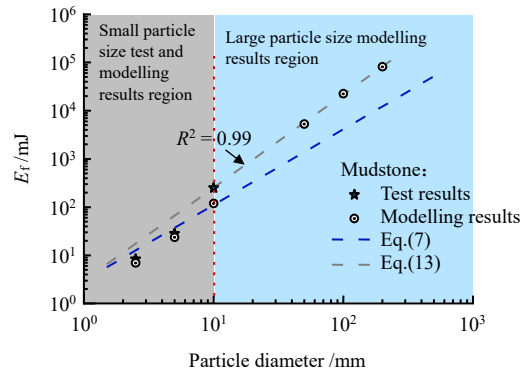
(b) Average crushing strength comparison between the modelling and prediction results of the sandstone single particle

Fig. 13 Average crushing strength comparison between the numerical results and the predicted results of the large single particle

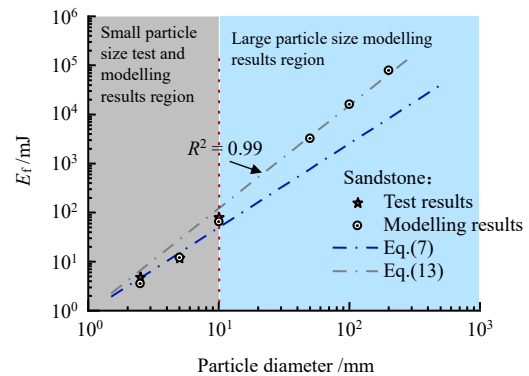
The comparison of the average crushing strength between the modelling results and the theoretical results of mudstone and sandstone is shown in Figs.13a and 13b, respectively. For large particle size, it is seen from Fig.13 that the numerical results of the average crushing strength agree well with those calculated from Eq.(4). As the particle size increases, the crushing force continuously increases

and the crushing strength decreases. In this way, the particle fractal dimension D and E.(4) can be used to predict the crushing strength of a single particle with a large particle size. However, as the particle size continues to increase, the average crushing strength of the single particle does not decrease indefinitely, and the specific results need to be further verified by more laboratory experiments.

The changing trend of the average crushing energy of single particles of mudstone and sandstone is shown in Figs.14a and 14b, respectively. As seen from Fig.14 that as the increase of particle size, the crushing energy also increase, which shows a similar trend as the previous discussion. However, there is a somewhat different between the numerical modelling results and the theoretical prediction results by Eq.(7). As for the small particle size (the grey area in Fig.14), the numerical modelling gives reasonable results, which are consistent with the predicted results. As for the large particle size (the light blue area in Fig.14), the Eq.(7) seems not suitable to predict the results and the numerical modelling results are larger than that of the predicted results.



(a) Average crushing energy comparison between the modelling and prediction results of the mudstone single particle



(b) Average crushing energy comparison between the modelling and prediction results of the sandstone single particle

Fig. 14 Average crushing energy comparison between the numerical results and the predicted results of the large single particle

According to the numerical modelling results, Eq.(7) is then modified and it is found that there is a certain

regularity in its changing:

$$E_f \propto d^{A\left(\frac{5D}{3}-2\right)} \quad (13)$$

where A is a fitting parameter, which is selected as 1.23. In this manner, the Eq.(7) is used to predict the crushing energy for the small particle size (the grey area in Fig.14), while for large particle size (the light blue area in Fig.14), Eq.(13) is then used for a proper prediction of crushing energy. Hence, the particle fractal dimension D and Eq.(13) can be used to predict the crushing energy of single particle with large particle sizes.

7 Conclusion

Based on the size effect on the strength and deformation behaviour of coarse-grained soil, the fractal dimension, particle strength, crushing energy, and Weibull distribution of single particles were studied by using single particle crushing tests of mudstone and sandstone samples with different particle sizes in this study. The test results were then verified and analyzed through numerical modelling using the DEM code PFC^{3D}. Based on the results, the crushing strength and energy of large particle sizes can be predicted. The main conclusions from this study are as follows:

(1) Under the same particle size condition, the sandstone fragmentation is larger than that of the mudstone. Under the same test conditions, the fractal dimension is different between the mudstone and sandstone. For the coarse-grained soil, only the fractal dimension determined by the same test can be used to predict the mechanical properties of the same material. In the single particle crushing tests, the fractal dimensions of the mudstone and sandstone are 2.14 and 2.22, respectively.

(2) In this study, under the same single particle test conditions, the strength of the mudstone is higher than that of the sandstone. It is found from the single particle tests that the crushing strength obeys the size effect. The larger the particle size, the smaller the crushing strength. The crushing energy of single mudstone particle is greater than that of the sandstone, and the larger the particle size, the greater the crushing energy. The crushing strength and energy of single particle can be predicted using the fractal dimension.

(3) The single particle crushing test shows that the particle crushing strength of coarse-grained soil follows the Weibull distribution. The Weibull modulus obtained by Eq.(9) is consistent with the modified Weibull modulus calculated by Eq.(11). The Weibull modulus of granular materials can be calculated using the fractal dimension D and Eq.(11).

(4) Based on the modelling results of DEM PFC^{3D} numerical simulation, the crushing strength of a single particle can be calculated by the fractal dimension D and Eq.(4). The crushing energy of a single particle, Eq.(13)

is more appropriate than Eq.(7), it is therefore to use the fractal dimension D and Eq.(13) to derive crushing energy of single particle. In addition, it should be mentioned that only the modelling results are considered herein for single particles with large particle sizes, and the specific results need to be further verified by more laboratory experiments.

References

- [1] INDRARATNA B, SALIM W. Modelling of particle breakage of coarse aggregates incorporating strength and dilatancy[J]. *Geotechnical Engineering*, 2002, 155(4): 243–252.
- [2] VARADARAJAN A, SHARMA K G, VENKATACHALAM K, GUPTA A K. Testing and modeling two rockfill materials[J]. *Journal of Geotechnical and Geoenvironmental Engineering*, 2003, 129(3): 206–218.
- [3] INDRARATNA B, THAKUR P K, VINOD J S. Experimental and numerical study of railway ballast behavior under cyclic loading[J]. *International Journal of Geomechanics*, 2010, 10(4): 136–144.
- [4] XIAO Y, LIU H. Elastoplastic constitutive model for rockfill materials considering particle breakage[J]. *International Journal of Geomechanics*, 2017, 17(1): 04016041.
- [5] HARDIN B O. Crushing of soil particles[J]. *Journal of Geotechnical Engineering*, 1985, 111(10): 1177–1192.
- [6] ZHOU Hai-juan, MA Gang, YUAN Wei, et al. Size effect on the crushing strengths of rock particles[J]. *Rock and Soil Mechanics*, 2017, 38(8): 2425–2433.
- [7] WANG Feng, ZHANG Jian-qing. Study of breakage behaviour of original rockfill materials considering size effect on particle strength[J]. *Rock and Soil Mechanics*, 2020, 41(1): 87–94.
- [8] FROSSARD E, HU W, DANO C, et al. Rockfill shear strength evaluation: a rational method based on size effects[J]. *Geotechnique*, 2012, 62(5): 415–427.
- [9] NAKATA Y, KATO Y, HYODO M, et al. One-dimensional compression behavior of uniformly graded sand related to single particle crushing strength[J]. *Soils and Foundations*, 2001, 41(2): 39–51.
- [10] MCDOWELL G R, AMON A. The application of Weibull statistics to the fracture of soil particles[J]. *Soils and Foundations*, 2000, 40(5): 133–141.
- [11] LIM W L, MCDOWELL G R, COLLOP A C. The application of Weibull statistics to the strength of railway ballast[J]. *Granular Matter*, 2004, 6(4): 229–237.
- [12] WANG W, COOP M R. An investigation of breakage behaviour of single sand particles using a high-speed microscope camera[J]. *Geotechnique*, 2016, 66(12): 1–15.
- [13] CUNDALL P A, STRACK O D L. A discrete numerical-model for granular assemblies[J]. *Geotechnique*, 1979, 29(1): 47–65.
- [14] MCDOWELL G R, HARIRECHE O. Discrete element

- modelling of soil particle fracture[J]. *Geotechnique*, 2002, 52(52): 131–135.
- [15] CIANTIA M O, ARROYO M, CALVETTI F, et al. An approach to enhance efficiency of DEM modelling of soils with crushable grains[J]. *Geotechnique*, 2015, 65(2): 91–110.
- [16] CIANTIA M O, ARROYO M, BUTLANSKA J, GENS A. DEM modelling of cone penetration tests in a double-porosity crushable granular material[J]. *Computers and Geotechnics*, 2016, 73: 109–127.
- [17] ZHANG Cheng-gong, YIN Zhen-yu, WU Ze-xiang, et al. Three-dimensional discrete element simulation of influence of particle shape on granular column collapse[J]. *Rock and Soil Mechanics*, 2019, 40(3): 1197–1203.
- [18] ZHOU Meng-jia, WEN Yan-feng, DENG Gang, et al. Three-dimensional discrete element simulation of random breaking strength and size effect in single particle splitting test of rockfill[J]. *Rock and Soil Mechanics*, 2019, 40(Suppl.1): 503–510.
- [19] XU Kun, ZHOU Wei, MA Gang, et al. Review of particle breakage simulation based on DEM[J]. *Chinese Journal of Geotechnical Engineering*, 2018, 40(5): 880–889.
- [20] MANDELBROT B B. *The fractal geometry of nature*[M]. San Francisco: W.H. Freeman, 1983.
- [21] CHI Shi-chun, WANG Feng, JIA Yu-feng, et al. Modeling particle breakage of rockfill materials based on single particle strength[J]. *Chinese Journal of Geotechnical Engineering*, 2015, 37(10): 1780–1785.
- [22] XU Yong-fu. Theory of shear strength of granular materials based on particle breakage[J]. *Chinese Journal of Geotechnical Engineering*, 2018, 40(7): 1171–1179.
- [23] MCDOWELL G R, BOLTON M D. On the micromechanics of crushable aggregates[J]. *Geotechnique*, 1998, 48(5): 667–679.
- [24] XU Y F. Explanation of scaling phenomenon based on fractal fragmentation[J]. *Mechanics Research Communications*, 2005, 32(2): 209–220.
- [25] EINAV I. Breakage mechanics—part I: theory[J]. *Journal of the Mechanics and Physics of Solids*, 2007, 55: 1274–1297.
- [26] XIAO Y, MENG M Q, DAOUADJI A, et al. Effect of particle size on crushing and deformation behaviors of rockfill materials[J]. *Geoscience Frontiers*, 2019, <https://doi.org/10.1016/j.gsf.2018.1010.1010>.
- [27] MENG M Q, SUN Z C, WANG C G, et al. Size effect on mudstone strength during freezing-thawing cycle[J/OL]. *Environmental Geotechnics*, 2020: 1–16, (2019-10-30) [2019-12-17] <https://doi.org/10.1680/jenge.1618.00160>.
- [28] WANG Y, SHAO C, XU Y. Fractal crushing of solid particles[J]. *KSCE Journal of Civil Engineering*, 2017, 21(3): 987–993.
- [29] XU Y F, XU J P, WANG J H. Fractal model for size effect on ice failure strength[J]. *Cold Regions Science and Technology*, 2004, 40(1-2): 135–144.
- [30] JAEGER J C. Failure of rocks under tensile conditions[J]. *International Journal of Rock Mechanics and Mining Sciences*, 1967, 4(2): 219–227.
- [31] WEIBULL W. A statistical distribution function of wide applicability[J]. *Journal of Applied Mechanics*, 1951, 13(2): 293–297.
- [32] JAYATILAKA A D S, TRUSTRUM K. Statistical approach to brittle fracture[J]. *Journal of Materials Science*, 1977, 12(7): 1426–1430.
- [33] GUIDA G, BARTOLI M, CASINI F, et al. Weibull distribution to describe grading evolution of materials with crushable grains[J]. *Procedia Engineering*, 2016, 158: 75–80.
- [34] ZHANG Zong-tang, GAO Wen-hua, ZHANG Zhi-min, et al. Evolution of disintegration breakage of red sandstone particles using Weibull distribution[J]. *Rock and Soil Mechanics*, 2020, 41(3): 1–10.
- [35] GREGORY J. The density of particle aggregates[J]. *Water Science and Technology*, 1997, 36(4): 1–13.
- [36] NAKATA A F L, HYDE M, HYODO H. A probabilistic approach to sand particle crushing in the triaxial test[J]. *Geotechnique*, 1999, 49(5): 567–583.